Int. J. of GEOMATE, Dec., 2014, Vol. 7, No. 2 (Sl. No. 14), pp. 1062-1069
Geotech., Const. Mat. and Env., ISSN:2186-2982(P), 2186-2990(O), Japan

NUMERICAL SIMULATION OF RIGID PAVEMENT BEHAVIOR TO NON-DESTUCTIVE IMPULSE RESPONSE TESTING

Hudson Jackson[1] and Kassim Tarhini[1]

[1]United States Coast Guard Academy, United States of America

ABSTRACT: The Impulse Response (IR) technique is a stress wave method that measures the structure's response to stress waves generated by an impact source. When applied to rigid pavements, the measured response contains complex information on the dynamic pavement properties that is primarily used in detection of voids or loss of support, and softening of the subgrade. The dynamic response of the pavement system is assumed to be similar to that of a single degree of freedom (SDOF) system. This assumption is useful for practical purposes but introduces inconsistencies and uncertainties in the data interpretation because it oversimplifies a complex dynamic problem. Results of a Finite Element parametric study analysis conducted to identify key factors that influence rigid pavement response during Impulse Response (IR) testing are presented. A dynamic modal analysis of a multilayer rigid pavement, assuming viscoelastic and elastic linear material properties, indicates that the mobility spectra from IR testing is predominantly influenced by the properties of the surface layer and the subgrade. The presence of voids beneath a rigid pavement results in increased mobility and less damped behavior of the pavement. The validity of the SDOF assumption in void detection in the reduction of field IR data is also examined.

Keywords: *Impulse response, Rigid pavement, Nondestructive testing, Voids, Flexibility spectrum, Finite element, Mobility*

1. INTRODUCTION

The Impulse Response (IR) method is a surface reflection method that depends on the propagation of stress wave through the pavement system. The pavement is excited by an impact and the response measured. There are generally three major types of waves in an elastic half-space that are of interest for pavement testing, namely; compression (P), shear (S) and Rayleigh (R) waves. The nature of an impact and the medium of propagation determine which wave dominates. Compression or P-waves are of primary interest in impulse response testing. They are the fastest of all the waves with particle oscillation in the direction of the wave propagation. They can travel through any type of medium and subject the particles to alternate compressional and tensile stresses as the wave travels through the medium. In any form of seismic testing, P-waves are the first to arrive at the receivers; their arrival can be distinguished by displacements in the form of oscillations. In a layered half-space, with two or more layers, the waves undergo reflections and refractions at each interface. The extent to which the incident wave is reflected or transmitted depends on the angle of incidence, the ratio of wave velocities and the ratio of densities of the media [1]. Changes in the wave velocity, density or elastic modulus causes an impedance change. The fraction of the incident wave that is reflected from an interface is dependent on the impedances of both media.

Pavement systems can be considered as layered elastic systems. Waves generated by an impact travel through the structure producing disturbances within the pavement. The disturbances are generally small and in the elastic range; the effects can therefore be considered in terms of the propagation of elastic stress waves within the pavement. The generated waves are generally composed of widely distributed frequency components. The nature of the stress waves generated determines their ability to propagate through the various pavement materials and their ability to detect defects in the pavement system. For example, when a void is present, most of the energy is reflected from the void-pavement layer interface. The wavelength of the propagating wave determines the ability of the Impulse Response method to detect defects within the pavement. In general, defects on the order of, or greater than, the wavelength of the propagating wave can be fully detected. The interaction of stress waves with internal discontinuities critically depends upon the relationship between wavelength and the dimensions and depth of the discontinuity [2].

The interpretation of IR data is a complex process because the frequency response of the pavement depends on the type and rate of loading, temperature, and the state of stress and properties of the individual pavement layers. Therefore, dynamic models are required to accurately evaluate pavement response under nondestructive testing conditions. The current IR data reduction procedure simplifies the dynamic response of the pavement-soil system to that of a single degree of freedom (SDOF) system. Curve fitting between the actual response and that of a SDOF system is done to obtain the necessary modal parameters. The assumption of a SDOF response oversimplifies the problem and, although useful for practical purposes, introduces inconsistencies and uncertainties in the data interpretation [3]. The results obtained from the SDOF simulation are not always

representative of the actual response of the pavement-soil system depending on the vibration mode, properties of the supporting soil and characteristics (geometry, rigidity) of the pavement due to a complex variation of stiffness and damping coefficient with frequency.

In order to investigate the validity of the assumption of the SDOF response and to improve data interpretation of the IR method used in the Seismic Pavement Analyzer [4, 5], a finite element based parametric study of factors affecting the response of rigid pavements with and without voids was conducted. Results from the simulation are presented in terms of mobility and stiffness spectra. The first part of the paper discusses fundamentals of the IR technique used in pavement condition assessment. The second part deals with the finite element simulation of the IR test and effects of various parameters on the response and mobility spectra.

2. OVERVIEW OF THE IMPULSE RESPONSE METHOD

The Impulse Response method also known as the Transient Dynamic method is a nondestructive testing method that is used in quality control and condition assessment of pavements and deep foundations. The method was first developed in France in the late 1970's as an extension of the vibration test, which was used in the quality control of drilled shafts constructed in France [6]. The IR method has been successfully used to determine the subgrade modulus and presence of voids or loss of support in rigid pavements [4, 5].

2.1 Field Testing

The pavement is first divided into square grids and testing is done at the corner of each grid. The pavement is excited and the response measured at a nearby location. Spectra for both impact and response (particle velocity) are combined to obtain either the mobility, flexibility or impedance function of the pavement. IR testing was incorporated into a device called the Seismic Pavement Analyzer (SPA). The SPA, shown in Fig. 1, is a device for nondestructive testing (NDT) of pavements, developed at the University of Texas at El Paso under the Strategic Highway Research Program [3]. Five different wave propagation techniques (spectral analysis of surface waves, impact echo, ultrasonic body waves, ultrasonic surface waves and impulse response) are incorporated into this device. The IR test done with the SPA uses the low frequency impact source and a nearest geophone G1, 25 cm away (Fig. 1). The rigid pavement is impacted to couple stress waves energy in the surface layer. A portion of the energy is reflected at the slab-base interface and a portion is transmitted to the subgrade. The load cell at the tip of the low frequency source records the impact energy, while the response, in terms of the particle velocity, is recorded by geophone G1.

2.2 Data Reduction and Interpretation

The recorded load and velocity histories are then transformed to the frequency domain using a Fast-Fourier Transform algorithm. At each frequency, the ratio of load to velocity, termed mobility, is determined. The mobility is integrated to obtain the stiffness. The mobility of pavement slabs with good support is fairly uniform up to a frequency of about 600 Hz, while a pavement with voids or loss of support has multiple resonant peaks.

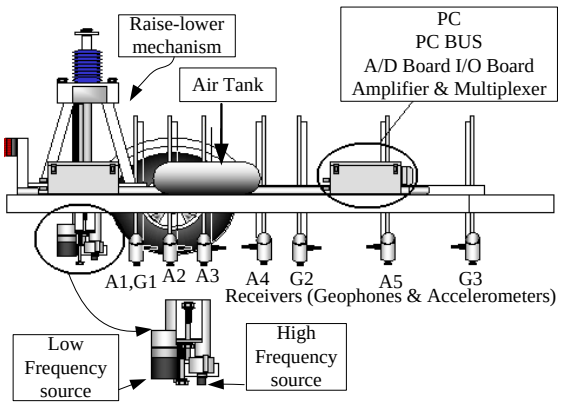

Fig. 1 Schematic of the Seismic Pavement Analyzer.

The underlying assumption of the IR method is that a rigid pavement system can be approximated by a response of a SDOF system, with the controlling stiffness being that of the subgrade. The response curve contains the information needed to determine the dynamic stiffness and shear modulus of the subgrade used in quality control/condition assessment of the pavement. The use of the IR technique for determination of the subgrade modulus is illustrated in Fig. 2. Both the load and time histories and corresponding spectra are obtained from a load cell and a close low-frequency geophone (G1) respectively. The dynamic stiffness spectrum, representing the ratio of the two (load and displacement) spectra is matched by the response spectrum of a single degree of freedom system. The modal parameters of the SDOF system: the natural frequency, static stiffness and damping ratio are obtained to characterize the pavement. The natural frequency and static stiffness are used to evaluate the shear modulus, and the mobility and damping characteristics to detect voids or loss of support.

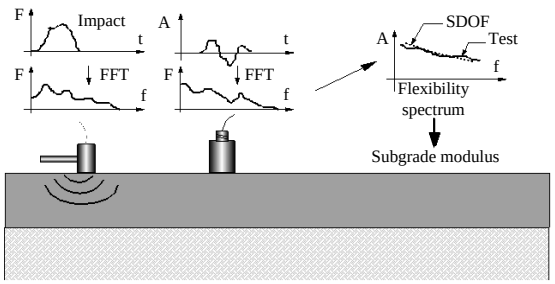

Fig. 2 Evaluation of subgrade modulus by the IR technique

Detection of loss of support due to presence of voids underneath rigid pavements relies on a change in the pavement mobility. When voids are present, a significant portion of the wave energy is reflected back to the surface, resulting in an increase in mobility and a less damped response. Response of a slab with good support or sound contact can be described as a highly damped response, because a large portion of the impact energy can be radiated towards the interior of the medium. On the other hand, voids cause the energy to be trapped within the slab, resulting in a low damped response. Loss of support or voids beneath joints of a slab is typically indicated by a damping ratio in a range of 10 to 40%, while loss of support beneath the middle of a slab is typically indicated by a ratio in a range of 30 to 60% [3].

3. FINITE ELEMENT PARAMETRIC STUDY

The Finite Element Method (FEM) provides an excellent tool for simulating and studying the response of a pavement multilayered system to dynamic loading induced by IR testing. Response of a rigid pavement to a dynamic load is affected by the properties of the concrete slab and the supporting base and subgrade. A parametric study was conducted to investigate the influence of factors such as pavement dimensions, Poisson's ratio, elastic modulus and flexural rigidity of the slab; layer thicknesses, elastic modulus of the base layer, the elastic modulus of the subgrade, and depth to bedrock on the dynamic response of a rigid pavement subjected to IR loading. A commercially available finite element program, ABAQUS was used in the simulation.

3.1 Rigid Pavement Model Geometry

The cross section and pavement layer properties are shown in Fig. 3. The pavement is modeled as a multilayered viscoelastic system. It is treated as a plane strain problem, symmetrical with respect to the point of load application. The finite element model is discretized using 8-node biquadratic plane strain elements of a 10cm width in the horizontal direction. In the vicinity of the load, the mesh is refined using smaller elements. Both the concrete slab and base layers are discretized by 3 rows of elements each. Two finite element models, shown in Figs. 4 and 5, were used. In both models, the same mesh discretization and element type for the concrete slab and base layer are used. Model 1 consists of a subgrade comprising of 50 rows of 8-node biquadratic plane strain elements. Four-node plane strain infinite elements are used in the description of the subgrade in both models. Using infinite elements eliminates the need to truncate the infinite domain and provide a means of effectively modeling extensive subgrade soil layers [7]. Model 1 represents a pavement supported on a uniform subgrade of finite thickness (stiff layer at a depth of 4.95 m). Model 2 better represents a half-space of infinite depth underneath a pavement.

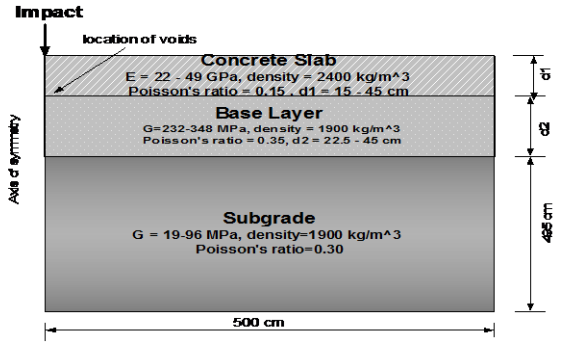

Fig. 3 Cross section and material properties of three-layer rigid pavement

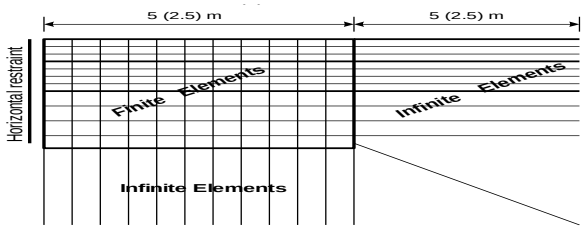

Fig. 4 Schematics of FE Model 1

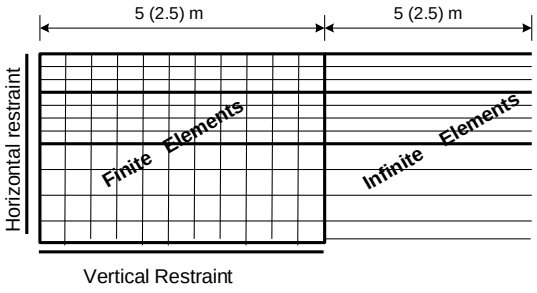

Fig. 5 Schematics of FE Model 2

3.2 Loading and Frequency Resolution

The loading was approximated by a Haversine function of 1.6 ms duration and maximum force of 5kN. This impact loading function was selected because it closely describes a typical hammer impact of the Seismic Pavement Analyzer (SPA). Time integration of 0.8 ms with 2048 increments was used, providing a maximum frequency of 625 Hz with a 0.61 Hz resolution ($1/10^{th}$ that obtained from the SPA) data. A lower resolution was used to obtain more information in the lower frequency range of the stiffness spectra.

3.3 Layer Properties

The strain level induced in the pavement layers during IR testing is very low. Therefore, materials of all the layers are described as linearly elastic. Each pavement layer is described by its shear modulus (shear wave velocity), mass density and Poisson's ratio. Damping is described as a Rayleigh type damping, with Rayleigh constants β and α equal to 0 s^{-1} and 10^{-3} s, respectively. It is usually difficult to accurately model the damping of a structure. In this study, the maximum frequency of interest was about 600 Hz and the lowest frequency, 0 Hz. The relationship between the damping ratio, ξ for a single mode of vibration, angular frequency ω, and Rayleigh damping is given by:

$$\xi = \frac{\beta}{2\omega} + \frac{\alpha\omega}{2} \qquad (1)$$

Substituting these values β = 0 s^{-1} and α = 10^{-3} s into Rayleigh damping equation yields a damping ratio of 0 – 30 %. The damping ratio for the models was assumed to be in this range.

Voids were simulated by defining them as thin cracks, or by a removal of already generated elements. When described as cracks, voids were defined by two sets of elements above and below the crack connected to two sets of nodes of the same coordinates, but without a direct connection. The ranges of properties investigated are shown in Fig. 3 and summarized in Table 1.

Table 1. Range of Pavement Parameters Investigated

Parameter	Range of values
Slab Thickness [cm]	15, 22.5, 30, 45
Base layer thickness [cm]	0, 15, 22.5, 30, 45
Young's modulus of concrete slab [GPa]	22, 35, 50
Shear modulus of base layer [MPa]	232, 300, 385
Shear modulus of subgrade [MPa]	19, 76, 120
Depth to bedrock [m]	2.5, 5, 10, 25

4. RESULTS AND DISCUSSION

The absolute mobility and stiffness spectra 25 cm (similar to the location of geophone G1 in the SPA) from the impact source are shown in Figs. 6 and 7. The mobility for model 1 and model 2 with H/R = 10, increases with frequency and then decreases after reaching a peak value. The absolute stiffness generally increases with frequency. These trends are identical to that observed from IR field results from SPA testing. The mobility for both models are uniform for high values of depth to bedrock/width (H/B) ratios—i.e. deeper depths to bedrock.

The mobility and stiffness for model 1 and model 2 (with H/B =10, implying extensive depth to bedrock) being similar is an indication that infinite elements suitable represent the subgrade as a half-space with no depth limitation. For model 2 with H/R =2 (implying shallow bedrock), multiple peaks are observed in the absolute mobility and stiffness spectra. Due to a slight rigid body motion caused by the use of infinite elements, a small static component is introduced resulting in a nonzero mobility at zero frequency (Fig. 7). Two prominent peaks at 17 Hz and 44 Hz, corresponding to the natural frequency of the subgrade to shear and compression waves, respectively, are evident in the mobility spectra of model 2 with H/R = 2 (Fig. 6). The quiet boundary provided by the infinite elements reduces the reflection back into the finite element model. It appears that the first peak (at 17 Hz) in the mobility spectrum is related, to a certain degree, to the amount of reflections within the model.

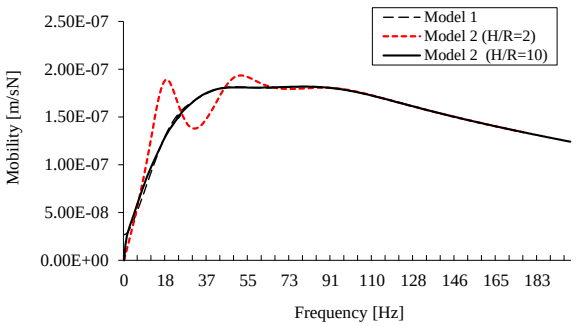

Fig. 6 Typical mobility spectra for models 1 & 2

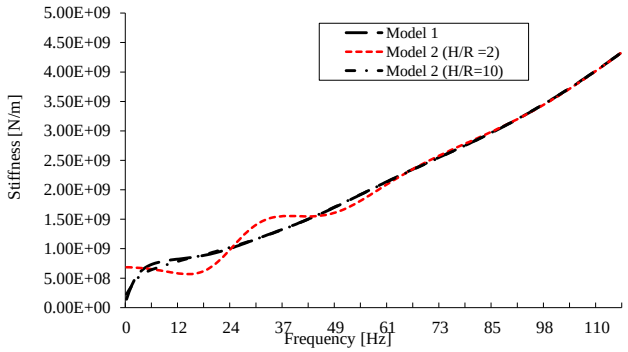

Fig. 7 Typical absolute stiffness spectrum

For a harmonic excitation, an analogy can be drawn between a SDOF oscillator and a massless 3D foundation on an elastic half-space [9]. The dynamic stiffness or impedance S(ω) (for a particular frequency) is given by the following equations.

$$\boldsymbol{S(\omega) = K - \omega^2 M + i\omega C} \qquad (2)$$

$$\boldsymbol{S(\omega) = K_s\left[\left(1 - \frac{\omega^2}{\omega_n^2}\right) + i2\beta_d \frac{\omega}{\omega_n}\right]} \qquad (3)$$

Where, β_d is the critical damping ratio, ω_n the natural frequency, and K_s the static stiffness of the slab–soil system.

The shear modulus of the subgrade can be calculated based on its relationship with static stiffness (Eq. 4) developed for a rigid circular foundation resting on a homogeneous half-space [10].

$$\boldsymbol{K_s = \frac{4GR_e}{1-\upsilon}} \qquad (4)$$

Where, G is the subgrade shear modulus, R_e the equivalent radius, and υ Poisson's ratio of the soil.

Since pavement slabs are circular, K_s must be corrected by applying a shape correction factor to account for the effect of length to breadth ratio on dynamic stiffness [10]. It can be seen from Eq. 2 and Eq. 3 that dynamic stiffness of a SDOF system varies as a second degree parabola with the first part representing the spring function (real part of spectrum) and the second, the damping function (imaginary part of spectrum). By measuring the impedance, the parameters needed to characterize the system such as static stiffness, damping ratio and natural frequency, the appropriate pavement properties can be determined. The typical variation of spring function with frequency for model 2 is shown in Figure 8. In general spring function for both models increases and then decreases with increasing frequency. This trend is observed in field data of rigid pavements collected with the SPA and is also typical for rectangular footings on a homogeneous half-space [11].

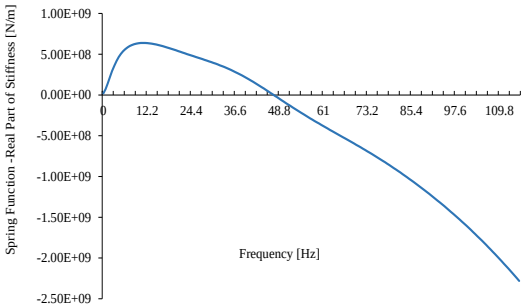

Fig. 8 Typical spring function spectrum for Model 2

4.1 Influence of Flexural Rigidity of Concrete Slab

Effects of slab thickness, d_1, and Young's Elastic Modulus, E_{sl}, can be combined into a flexural rigidity (FR) of the slab given by Eq. 5.

$$FR = E_{sl}d_1^3/12(1 - \nu^2) \qquad (5)$$

The range of slab thickness and Young's modulus investigated are shown in Table 2 as well as the corresponding dimensionless stiffness ratios (SR), defined as:

$$SR = FR/G_sR_e^3 \qquad (6)$$

Where, G_s is the shear modulus of the subgrade and R_e is the equivalent radius of the concrete slab.

SR represents the relative flexural rigidity of the concrete slab to that of the soil subgrade.

Table 2 Range of flexural rigidity and stiffness ratio

Slab thickness d_1 [m]	Elastic Modulus of slab E_{sl} [GN/m^2]	Flexural rigidity FR [MNm]	Stiffness Ratio SR x10^{-3}
0.150	22	6.33	1.2
0.150	34.5	9.92	1.9
0.150	49.7	14.3	2.7
0.225	22	21.4	4.0
0.300	22	50.6	9.6
0.450	22	171	32.4

Note: Shear modulus of subgrade and base = 76 and 232 MN/m^2, respectively

In general, mobility decreases with increasing flexural rigidity or stiffness ratio. Mobility is more sensitive to changes in flexural rigidity due to changes in slab thickness than to changes in Young's modulus. This is evident from Eq. 5; flexural rigidity varies with thickness to the third power. There is a general increase in stiffness with flexural rigidity with change more pronounced at higher frequencies. The static stiffness, K_s was normalized to that of a "*typical*" rigid pavement. For the purpose of this study, the typical or standard rigid pavement was defined as one with a 450 mm slab, slab elastic modulus of 22 GPa, shear modulus of base layer and subgrade of 232 MPa and 76 MPa, respectively (i.e, flexural rigidity ≥ 170MNm, SR ≥ 0.032). There is negligible change in static stiffness with increasing stiffness ratio. There was only a 1% change in static stiffness over the range of stiffness ratios investigated for model 1. The changes in static stiffness becomes more significant with decreasing H/B ratio for model 2. The variation of normalized static stiffness is shown in Fig. 9 for

model 1. Similar trends were observed for the individual variation of H/B ratios.

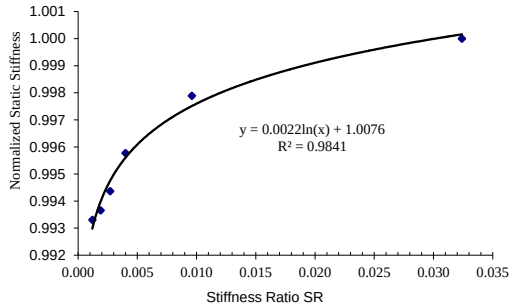

Fig. 9 Variation of normalized static stiffness with slab-subgrade stiffness ratio-model 1

Peak (maximum) mobility decreases logarithmically with increasing slab flexural rigidity and slab-subgrade stiffness ratio as shown in Fig. 10 for model 2. Similar curves were obtained for both models. However, model 2 is more sensitive to changes in the flexural rigidity of the slab due to the effect of the depth to bedrock on wave propagation within the pavement layers.

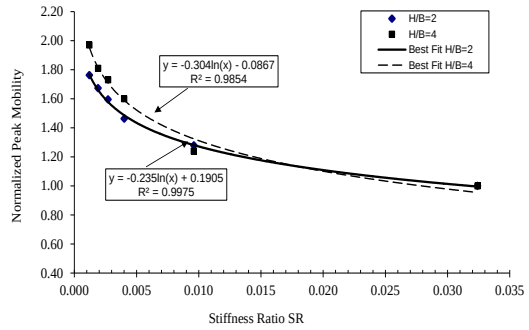

Fig. 10 Variation of peak mobility with slab-subgrade stiffness ratio-model 2

4.2 Influence of Shear Moduli of Base and Subgrade

The results are presented in terms of shear modulus ratio GR, *defined as the ratio of the shear modulus of the pavement base layer to that of the subgrade.* Six different values of GR ranging from 2.0 to 12.0 were investigated. The effects of changes in both the shear modulus of base and subgrade were investigated by varying one while the other was held constant. The shear modulus of the base was held constant at 232 MN/m^2, while that of the subgrade was varied; this enabled the effects of subgrade shear modulus to be investigated. The shear modulus of the base layer (GR = 3, 4, and 5) was also varied while that of the subgrade was held constant at 76 MN/m^2.

The influence on the response due to changes in the shear modulus of the base layer are typically not significant. This is reflected in almost identical results for shear ratios of 3, 4 and 5 when G - of the base was changed. Static stiffness decreases with increasing shear modulus ratio. A high shear modulus ratio implies a weaker subgrade compared to the pavement base layer. One of the key assumptions of the IR data reduction for rigid pavements is that the subgrade, being the weakest layer, dominates the response. The static stiffness is therefore expected to decrease with decrease in the shear modulus of the subgrade. Both static stiffness and peak mobility were normalized to that of the already defined "typical" pavement system with a GR of 3. Typical variation of static stiffness with GR is shown in Fig. 11 for a stiffness ratio, SR of 0.0012. Static stiffness decreases logarithmically with GR. Similar trends were observed for other stiffness ratios for both models.

For GR = 12, which can be considered as a pavement with a weak subgrade support, more pronounced peaks in mobility were observed. These trends in mobility and stiffness are in agreement with the assumption that response to low frequency loading from IR testing is dominated by the quality of the subgrade support.

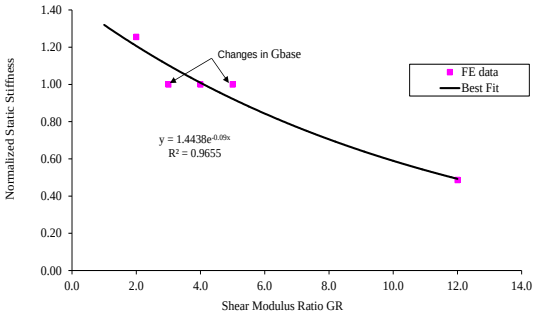

Fig. 11 Variation of static stiffness with base layer-subgrade shear modulus ratio-model 1 (SR=0.0012)

4.3 Influence of Thickness of Base Layer

Effects of the thickness of the base layer were investigated by varying it from 0 (slab on grade with no base layer) to 45 cm, while maintaining the slab thickness at a minimum thickness of 15 cm. The shear modulus of the base (G_b) and subgrade (G_s) were also held constant at 232 MN/m^2 and 76 MN/m^2, respectively (GR = 3.0). The results are expressed in terms of a dimensionless thickness ratio, TR, *defined as the ratio of thickness of the base layer to that of the concrete slab.*

Mobility decreases with increase in thickness ratio. As the thickness of the base layer increases, the stresses and strain induced in the subgrade reduces because it acts as a stress cushion. This reduction in both the strain and slab oscillation results in a decrease in overall mobility. Similar trends were observed for model 2. Both the static stiffness (SS) and peak mobility (PM) show a perfectly linear relationship with TR. SS increases while PM decreases linearly with TR. SS and PM, normalized with respect to the same for a pavement without a

base layer to develop dimensionless correlation parameters (not presented here due to space limitation). For the range of TR investigated, a 5% increase in static stiffness was observed for model 1 and 9% increase in model 2. These slight changes suggest that changes in base layer thickness do not have a profound effect on the static stiffness of the pavement-soil system. Peak mobility on the other hand, is more sensitive to changes in the thickness ratio. This implies that contribution of the base layer can be significant in some cases related to the mobility response and should not always be neglected in IR data reduction.

4.4 Influence of Depth to Bedrock

Changes in the response for model 2 due to the proximity of bedrock are shown in Fig. 12. The results are expressed in terms of H/B ratio, where H is the depth to bedrock and B is half the width of the pavement slab. Peak mobility increases with decreasing depth to bedrock. As expected, the static stiffness decreases with increasing depth to bedrock. For H/B = 10, the response approaches that of a pavement resting on a homogenous half-space. This is in agreement with work done by Gazetas, which suggests that, the response of a rigid circular disk on a stratum over a rigid base approaches that of the corresponding half-space for H/B = 8 [11]. The same trend is expected for rigid strip footings, but at higher H/B ratios.

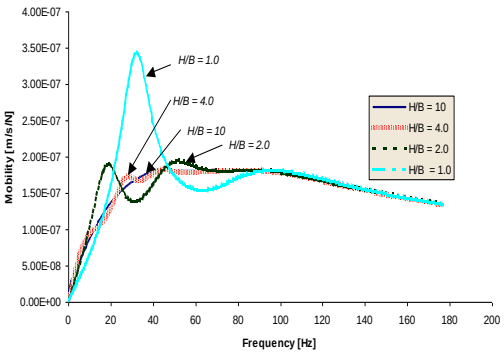

Fig. 12 Variation of absolute mobility spectra with H/B ratio-model 2

4.5 Influence of Voids

Three different void lengths, 60, 90 and 120 cm were introduced at the slab-base layer interface. The mobility at a distance of 25 cm from the load are presented in Fig. 13 for model 1. The mobility of the pavement-soil system increases with increasing void length, with a slight shift of the peak to higher frequencies.

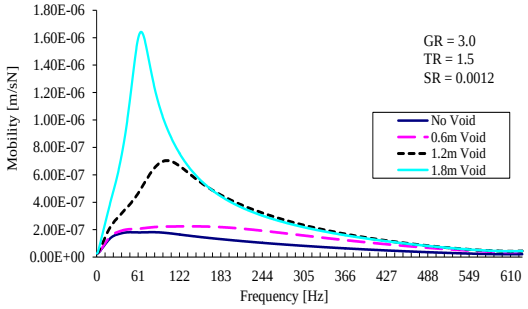

Fig. 13 Effect of void size on mobility for model 1

As void size increases, the peak mobility becomes more pronounced over a narrower frequency range. For model 2, as void length increases, the second peak becomes significantly higher than the first. This is due to a stronger reflection of stress wave from the voids before reaching the horizontal boundary. Both damping and spring function decrease with increasing void size. This is in agreement with findings of Nazarian *et al* [3] as well as field data collected on rigid pavements. Changes are more pronounced for the damping function. Most of the energy from the impact is reflected back to the surface resulting in a reduction of damping of the pavement system when voids are present.

This reduced damping implies higher displacements. If the loss of support is extensive, the slab tends to deform in a bending mode. Depending on the location of the void, and the magnitude of the impact, the slab deforms similar to a simply or fixed supported beam with multiple oscillations. In general, the spring function decreases with increasing void size. As void size decreases, the cross over frequency tends to increase, resulting in a reduction in natural frequency. It is evident from the results that the presence of voids or loss of support results in very significant changes in the mobility spectra.

5. VALIDATION OF THE SDOF ASSUMPTION

For a SDOF system, the displacement response increases with frequency up to a resonance peak and then decreases as frequency further increases. The response spectrum has of a single peak. The trends observed from the numerical simulation do not support a SDOF approximation in all cases, especially for values of H/B < 10, and large void sizes relative to the slab thickness. Multiple mobility peaks are evident for lower H/B ratios as well as for large voids. These trends are also observed in IR field data collected using the SPA. The mobility spectra from two rigid pavement sections, with poor support and good support, respectively are shown in Fig. 14. Multiple peaks are evident in the pavement with poor subgrade support.

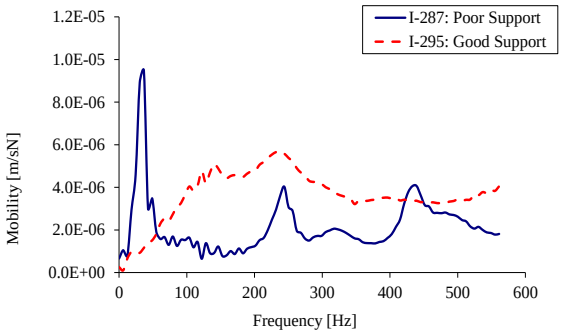

Fig. 14 Mobility spectra for rigid pavement with voids and good support

In general, mobility (velocity/load) as well as the flexibility (displacement/load) of the pavement increases with voids, resulting in a slight reduction of the fundamental frequency as the support deteriorates. This indicates that above a given void size, the fundamental response of the system, in vicinity of the void, is completely altered due to the changes in support conditions. This phenomenon cannot be fully captured by a SDOF model. Hoffmann and Thompson also back-calculated rigid pavement parameters by matching the measured and theoretical SDOF frequency response and reported error of up to 33% [12].

6. SUMMARY AND CONCLUSIONS

The results of a Finite Element parametric study conducted on a three layer rigid pavement models with unreinforced concrete slabs were presented. In general, the stiffness of the pavement system increases with increasing flexural rigidity of the concrete slab and thickness ratio, but decreases with increasing shear modulus ratio. Void or loss of support results in a significant increase in mobility and a reduction in the overall stiffness. Furthermore, significant differences in the response were observed for void lengths larger than double the thickness of the slab. As support conditions deteriorate, the fundamental response of the pavement is altered, resulting in the response being dominated by higher modes of vibration. The effect of the thickness of the base layer on pavement stiffness is less pronounced, but in some cases may affect the overall pavement mobility response significantly.

7. REFERENCES

[1] Richart, F.E. and Woods, R.D., "Vibrations of Soils and Foundations." Prentice-Hall, Inc., Englewood Cliffs, New Jersey, 1970.

[2] Sansalone, M.J. and Streett, W.B., "Impact Echo: Nondestructive Evaluation of Concrete and Masonry." Bullbrier Press, Jersey Shore, PA, 1997.

[3] Nazarian, S., Baker, M., & Crain, K. "Development and Testing of a Seismic Pavement Analyzer." Report SHRP-H-375, Strategic Highway Research Program, National Research Council, Washington, DC, 1993.

[4] Nazarian, S., Baker, M., & Reddy, S. "Determination of Voids Under Rigid Pavements Using Impulse Response Method." Nondestructive Testing of Pavements and Back Calculation of Moduli: Second Volume, STP 1198, ASTM Publication, Philadelphia, PA, 473-487, 1994.

[5] Gucunski, N., Vitillo, N. and A. Maher. "Pavement Condition Monitoring by Seismic Pavement Analyzer (SPA)." Structural Materials Technology IV–An NDT Conference, Atlantic City, New Jersey. 2000, pp337-342.

[6] Higgs, J.S. and Robertson, S.A. "Integrity Testing of Concrete Piles by Shock Method." Concrete, October 1979, pp. 31-33.

[7] Hjelmstad, K. D., Zuo, Q. and Kim, J. "Elastic Pavement Analysis Using Infinite Elements." Transportation Research Record 1568, Washington, DC.

[8] Cook, R. D., Malkus, D. S., and Plesha, M., E., "Concepts and Applications of Finite Element Analysis." 3rd edition, John Wiley and Sons Publishing Co., NY, 1989.

[9] Roesset, M., "Stiffness and Damping Coefficients of Foundations." Dynamic Response of Pile Foundations: Analytical Aspects, ASCE, New York, NY, 1980.

[10] Dobry, R., and Gazetas, G., "Dynamic Response of Arbitrary Shaped Foundations," ASCE Journal of Geotechnical Engineering, Vol. 112, No.2, New York, N.Y, 1986, pp109-135.

[11] Gazetas, G., "Analysis of Machine Foundation Vibrations: State of the Art," Soil Dynamics and Earthquake Engineering, Vol. 2, No. 1, 1983, pp 1-42.

[12] Hoffmann, M. S. and Thompson, M. R., "Mechanistic Interpretation of Nondestructive Pavement Testing Deflections" Transportation Engineering Series No. 32, University of Illinois, Urbana, 1981.

Int. J. of GEOMATE, Dec., 2014, Vol. 7, No. 2 (Sl. No. 14), pp. 1062-1069.
MS No. 4208 received on March 27, 2014 and reviewed under GEOMATE publication policies.

Corresponding Author: Hudson Jackson